The role of inelastic scattering in resonant tunnelling heterostructures

1991 J. Phys.: Condens. Matter 3 9087

(http://iopscience.iop.org/0953-8984/3/46/010)

J. Phys.: Condens. Matter 3 (1991) 9087–9101. Printed in the UK

The role of inelastic scattering in resonant tunnelling heterostructures

E V Anda† and F Flores
Departamento Física de la Materia Condensada, Universidad Autónoma de Madrid, Cantoblanco, 28049 Madrid, Spain

Received 3 January 1991, in final form 31 May 1991

Abstract. The non-equilibrium Keldysh formalism is used to analyse the role of the electron–phonon interaction in the transport properties of double-barrier heterostructures and microchannels in semiconductors. Elastic and inelastic contributions to the total current intensity are introduced and analysed as a function of the electron–phonon coupling; the elastic and inelastic intensities are related to the electronic spectrum and to the multiphonon excitations. The results obtained for the different mesoscopic systems considered compare well with the experimental evidence. The Keldysh formalism is shown to be very suitable to analyse many-body effects in mesoscopic systems.

1. Introduction

Transport in small semiconductor structures has been the subject of many studies in the last decade. These heterostructures are extremely attractive because of their very many technological applications. From an academic viewpoint the experimental study of their transport properties permits direct confrontation with theoretical results obtained using different formalisms and approximations for a great variety of conditions related with temperature, external magnetic and electric fields, dimension, disorder and many-body interactions (Büttiker 1988, Landauer 1989).

We are interested in addressing the effect that inelastic scattering and in particular the electron–phonon interaction has on the transport properties of these systems.

In the last few years, experimental measurements have shown clear evidence of the effect that the electron–phonon interaction has on the electrical current of mesoscopic systems. This is the case of the observed oscillatory behaviour of the electric conductance in semiconducting point contacts (Hickmott *et al* 1984, Lu *et al* 1985) and the appearance of satellites of the central resonant peak in a double-barrier resonant tunnelling experiment (Goldman *et al* 1987a, b). Non-thermal occupation due to a hot-carrier quantum distribution in semiconductor devices is another property which is mainly controlled by the electron–phonon interaction due to the mechanism through which electrons achieve thermodynamical equilibrium.

† Permanent address: Departamento de Física, Universidad Federal Fluminense, Outeiro de Sao Joao Batista s/n, Niteroi, RJ, Brazil.

0953-8984/91/469087 + 15 $03.50

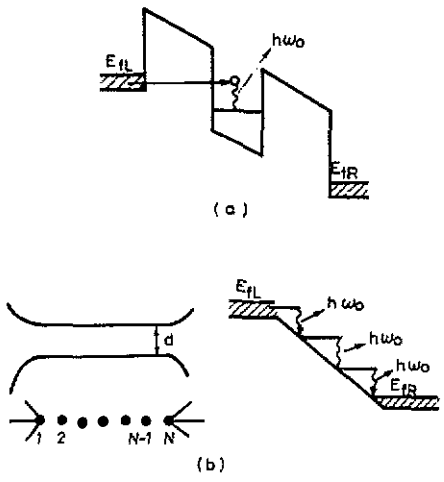

Figure 1. Heterostructures discussed in the paper: (*a*) potential well with a double-barrier heterostructure; (*b*) microchannel.

While inelastic scattering has been analysed before in mesoscopic systems, the approach has been mainly phenomenological (Büttiker 1986, Goldman *et al* 1987b, Yuming 1988). Recently, studies have appeared in the literature based on a simplified microscopic model which simulates a double-barrier heterostructure by a single-site energy level coupled to ideal leads and to phonons (Cai *et al* 1989, Jonson 1989, Wingreen *et al* 1989). Within the context of this model, resonant tunnelling in the presence of phonons has been studied either as a scattering problem through the calculation of the transmission matrix which implies knowledge of a two-particle Green function at the resonant site, or as a first-order tunnelling strength approximation using the tunnelling Hamiltonian formalism. Although these studies represent a significant contribution, it is difficult to generalize them in order to study real systems which need for their description many electronic and phonon states. This is particularly important when there is no spatially localized resonant level to be considered as is the case for multi-phonon processes in semiconductor mesoscopic channels. For these systems the scattering electron–phonon mean free path $L_{e\text{-}ph}$ is small in comparison with the microchannel length $L_{e\text{-}ph} \ll L$ (Kulik and Shekhter 1983). Here the electrical current can be thought of as being a diffusive drift of electrons which at certain sites is interrupted by the emission of an optical phonon. A theory capable of describing this situation requires a large number of states, at least one at each atomic site with position-dependent parameters. It is evident that such a description needs either a full self-consistent calculation of the electronic charge (Pernas *et al* 1990), or at least a plausible potential profile which depends upon the external bias.

The microscopic description of a system with many electronic and phonon states which incorporates the influence of inelastic scattering effects is crucial in order to understand the rich phenomenology associated with transport in mesoscopic systems. In particular, we mention the very interesting intermediate region between ballistic and macroscopic transport.

In this paper we present a microscopic approach to studying the effects of electron–phonon interaction on the transport properties of microsystems, based on a thermodynamical non-equilibrium formalism derived by Keldysh (1965). We shall follow the ideas proposed some time ago by Caroli *et al* (1971, 1972) in their study of tunnelling phenomena through insulating barriers. This formalism has several advantages. It

requires the calculation of only one-particle Green function, even for many-body systems; it gives exact results for the non-equilibrium independent-particle situation, and the many-particle effects can be calculated in principle to all orders in perturbation theory. Moreover, it provides all the tools to obtain in a self-consistent way the potential profile produced by the external bias. At this point, it should be commented that recent work by Datta (1990) and D'Amato and Pastawski (1989) has shown that the phenomenological approach followed by Büttiker to introduce dissipation via fictitious voltage probes can be related to the Keldysh formalism followed in this paper. Moreover, Chen and Ting (1990) used the Keldysh method to analyse other one-electron transport superlattice properties, and it is worth exploring this technique for systems with many-body interactions like the case considered here.

The paper is organized in the following way. In section 2 the microscopic model is presented. Sections 3 and 4 are dedicated to developing the formalism to be applied to study the transport of carriers under the effect of the electron–phonon interaction. We study the results obtained for the transport properties of double-barrier heterostructures and microchannels in semiconductors in sections 5 and 6. Finally section 7 is devoted to the summary and the conclusions.

2. The microscopic model

The heterostructures under study, as shown in figure 1, are described by the electron, phonon and electron–phonon Hamiltonians. The electronic part of the system is represented by the Hamiltonian

$$H_e = \sum_i \varepsilon_i n_i + \sum_{\substack{ij \\ \sigma}} t_{ij}(c_{i\sigma}^{+} c_{j\sigma} + \text{cc}) \tag{1a}$$

where ε_i is the site-dependent diagonal energy which models the microscopic characteristics of the heterostructure and the potential profile created by the stationary electronic charge that is accommodated according to the applied bias and the details of the structure. Although it is possible to obtain a self-consistent solution to this problem, for simplicity we shall assume that the applied bias produces a linear shift of the diagonal elements of the Hamiltonian along the sample.

In the direction perpendicular to the current flow, the system is assumed to possess translational symmetry such that $k_\parallel$ is a good quantum number. This will be the case of the double-barrier heterostructure. In the study of the point contact we shall suppose that the system is simply one dimensional. The off-diagonal matrix elements are taken between nearest neighbours. They are site dependent so as to be able to take into account the effective masses of the different semiconductors which form the heterostructure.

It is well known that a quantum well or more generally a thin film has a great variety of optical phonon modes (slab phonons) corresponding to bulk or interfaces excitations which have been observed experimentally (Shah 1986). Although the symmetry of these modes must be considered in order to explain the reduction in hot-electron relaxation in these devices in comparison with bulk materials, we shall neglect the influence of interfaces in the phonon spectra which will be taken to be 3D and completely flat. The main influence of this confinement is to reduce the strength of the interactions with electrons (Jain and Das Sarma 1989, Ridley 1989) which can be taken into account by renormalizing the electron–phonon interaction in relation to its bulk value. As a

consequence and for simplicity we assume that the Hamiltonian corresponding to the phonon degree of freedom is given by a sum of independent harmonic oscillators of frequency ω_0:

$$H_{ph} = \hbar\omega_0 \sum_i b_i^+ b_i. \tag{1b}$$

Finally the electron–phonon interaction is given by

$$H_{e\text{-}ph} = \sum_{i,\sigma} V_i c_{i\sigma}^+ c_{i\sigma}(b_i^+ + b_i) \tag{1c}$$

where in principle the interaction is extended to all the sample.

We have assumed that the optical phonons have a completely flat dispersion relation and that the electron–phonon interaction is local. This is justified because the velocity of propagation of a phonon is much less than the Fermi velocity; the phonon does not propagate much during the lifetime of the electronic fluctuation.

The theory that we develop is not restricted to any approximation concerning the contacts. We assume that the leads and its interaction with the heterostructure are represented by a one-electron Hamiltonian H_e. In practice the leads are modelled by two Bethe lattices with a coordination number $Z > 2$ which in practice operate as thermodynamical reservoirs of electrons with energies $\varepsilon < E_{FR}$ and $\varepsilon < E_{FL}$ for the right and left contacts respectively. For large values of Z this coincides with the bandwidth limit approximation which supposes that the bandwidth in the contacts is much larger than the characteristic energies of the system: the resonance width, the phonon energies, the applied voltage, etc.

3. The non-equilibrium formalism

The current circulating along a sample when an external bias is applied is in general a non-linear response phenomenon occurring in a system which is in non-equilibrium.

In view of the irreversible character of the tunnelling current, the usual perturbation theory does not apply and it is necessary to use a more general formalism capable of treating non-equilibrium processes. We adopt the Keldysh (1965) diagrammatic perturbation which requires the definition of a state of zero current flow which is obtained by partitioning the system at an arbitrary point such that each partition (left and right) has a Fermi level defined by E_{FL} and E_{LR} where the difference $E_{FL} - E_{FR}$ corresponds to the external applied voltage. This state is then used to build up an infinite diagrammatic expansion, taking as a perturbation the Hamiltonian which connects the two parts of the system. The diagrammatic expansion generated by this perturbation theory can be summed up without further difficulties and an exact result obtained as far as a single-particle system is concerned (Wingreen *et al* 1989). The effect of the interaction between particles can be incorporated into the theory using well known approximations provided by many-body theory.

In order to obtain the properties of the system, it is necessary to calculate non-equilibrium propagators which, following Keldysh formalism, are

$$-iG_{ij}^{-+}(t - t') = \langle c_i^+(t)c_j(t')\rangle \tag{2a}$$

$$iG_{ij}^{+-}(t - t') = \langle c_j(t')c_i^+(t)\rangle. \tag{2b}$$

The Fourier transform diagonal elements $G_{ii}^{-+}(\omega)$ and $G_{ii}^{+-}(\omega)$ are the spectral

representations of the state of occupation of site i for electrons and holes, respectively. The retarded and advanced Green functions, $G_{ij}^{R}(t-t')$ and $G_{ij}^{A}(t-t')$ respectively, give information on the distribution of available states of the system without any reference to their occupation.

In a similar way the propagators corresponding to phonons $D_{ij}^{-+}(t-t')$, $D_{ij}^{+-}(t-t')$, $D_{ij}^{R}(t-t')$ and $D_{ij}^{A}(t-t')$ are defined.

The propagators $G_{ij}^{+-}(\omega)$ and $G_{ij}^{R}(\omega)$ satisfy Dyson-type equations which are given by the formal equations (Keldysh 1965)

$$\mathbf{G}^{-+} = (\mathbf{1} + \mathbf{G}^{R}\boldsymbol{\Sigma}^{R})\mathbf{g}^{-+}(\mathbf{1} + \boldsymbol{\Sigma}^{A}\mathbf{G}^{A}) + \mathbf{G}^{R}\boldsymbol{\Sigma}^{-+}\mathbf{G}^{A}$$

$$\mathbf{G}^{R} = \mathbf{g}^{R} + \mathbf{g}^{R}\boldsymbol{\Sigma}^{R}\mathbf{G}^{R}.$$

For convenience, these equations are written in the following way:

$$\overset{-+}{G}{}_{ij}^{el}(\omega) = \{[1 + G^{R}(\omega)\Sigma^{R}(\omega)]g^{-+}(\omega)[1 + \Sigma^{A}(\omega)G^{A}(\omega)]\}_{ij} \tag{3a}$$

$$\overset{-+}{G}{}_{ij}^{incl}(\omega) = [G^{R}(\omega)\Sigma^{-+}(\omega)G^{A}(\omega)]_{ij} \tag{3b}$$

$$G_{ij}^{-+}(\omega) = \overset{-+}{G}{}_{ij}^{el}(\omega) + \overset{-+}{G}{}_{ij}^{incl}(\omega) \tag{3c}$$

$$G_{ij}^{R}(\omega) = g_{ij}^{R}(\omega) + [g^{R}\Sigma^{R}(\omega)G^{R}(\omega)]_{ij} \tag{3d}$$

with similar equations for $G_{ij}^{+-}(\omega)$ and $G_{ij}^{A}(\omega)$. Note that $\mathbf{G}^{-+}$ has been split into its elastic and inelastic parts (Caroli *et al* 1971, 1972) (see also below). The unperturbed propagators $g_{ij}(\omega)$ correspond to the system in thermodynamic equilibrium with a partition in it and without many-body interactions; $g^{-+}(\omega)$ and $g^{+-}(\omega)$ are simply given by

$$\overset{-+}{g}{}_{ij}^{+-}(\omega) = \mathrm{i}\,\mathrm{Im}\left(g_{ij}^{R}(\omega)\begin{Bmatrix} f(\omega) \\ 1-f(\omega) \end{Bmatrix}\right) \tag{3e}$$

where $f(\omega)$ is the Fermi distribution function. As will be discussed below, all the information on the inelastic processes are contained in the self-energy $\Sigma^{-+}(\omega)$. As a consequence the non-equilibrium propagator $G_{ij}^{-+}(\omega)$ can be expressed as the sum of $\overset{-+}{G}{}_{ij}^{el}(\omega)$ and $\overset{-+}{G}{}_{ij}^{incl}(\omega)$, the elastic and inelastic occupation spectra as given in equations (3).

The retarded and advanced self-energies $\Sigma^{R}(\omega)$ and $\Sigma^{A}(\omega)$ have two contributions:

(i) a local time one-particle self-energy which restores the eliminated connection between sites 1 and 2 (we are assuming that sites 1 and 2 are neither connected nor directly affected by many-body effects);

(ii) a many-body self-energy coming from the electron–phonon interaction.

In fact we are assuming that inelastic processes are restricted to a part of the system that can be isolated, i.e. to the well region for the case of a double-barrier heterostructure, or to the microchannels in semiconducting point contacts. Since the simultaneous treatment of the many-body interaction and the non-equilibrium situation is a difficult problem, it is tempting first to solve the many-body problem for the system isolated from the leads and then to tackle the non-equilibrium configuration of the system by linking it to the leads. Unfortunately, the electron–phonon interaction has not been included

in the zero-order propagator because creation and destruction operators of many-body states do not satisfy the Wick theorem, making the independent-particle diagrammatic expansion which re-established the connection in the system much more involved.

To calculate the self-energies $\Sigma^{R}(\omega)$ and $\Sigma^{-+}(\omega)$, standard many-body diagrammatic methods are used to sum infinite series obtained by perturbation theory. The Green function satisfies a Dyson equation with a vertex part, which according to Migdal (1958) is proportional to $1 + O(m/M)$ where m and M are the masses of the electron and the nucleus, respectively. Within the context of this theory, neglecting terms of the order of m/M in the self-energy $\Sigma^{R}_{ij}(\omega)$ describes the creation of a virtual phonon together with an electronic iso-energetic fluctuation. As the velocity of propagation of phonons is much less than the Fermi velocity, $\Sigma^{R}_{ij}(\omega)$ is short ranged and can be approximated by a local object.

If we restrict ourselves to spatial locality, $\Sigma^{-+}(\omega)$ can be written as follows:

$$\Sigma_i^{-+}(\omega) = \frac{iV_i^2}{2\pi}\int d\omega'\, D_{ii}^{-+}(\omega - \omega')G_{ii}^{-+}(\omega). \tag{4}$$

It is important to emphasize that the Green function $G_{ii}^{-+}(\omega)$ appearing in equation (4) corresponds to the propagator dressed by the electron–phonon interaction. The calculation of these quantities requires a self-consistent solution for G, Σ and D.

Great simplification is obtained if the dressed propagators in equation (4) are substituted by the undressed propagators, which reduces the expansion to second order in the electron–phonon interaction. This is normally a good approximation for semiconductors as is the case for resonant tunnelling in a double-barrier heterostructure, typically $GaAs/Al_xGa_{1-x}As$, for which the electron–phonon scattering mean free path is normally greater than the length of the sample along the electrical current direction. Then the satellite of the resonant tunnelling peak seen experimentally is a typical one-phonon process.

The optical phonon emission in ballistic transport detected in microchannels of InGaAs is, however, a very well characterized multi-phonon process. Its study requires one accordingly to consider higher-order corrections. This is done by taking the dressed electron propagator $G_{ii}^{+-}(\omega)$ in equation (4).

For the case of an optical phonon of frequency ω_0, $\Sigma_i^{-+}(\omega)$ is expressed by

$$\Sigma_i^{-+}(\omega) = (V_i^2/8\pi)[(1 + n_i)G_{ii}^{-+}(\omega + \omega_0) + n_i G_{ii}^{-+}(\omega - \omega_0)] \tag{5}$$

where n_i is the number of phonons present in the system at site i. In principle, n_i has to be obtained by integrating the phonon occupation spectral representation at site i. For simplicity we have taken the undressed phonon propagator to obtain equation (5) which gives

$$D_{ii}^{-+}(\omega) = (-i/4)[n_i\delta(\omega + \omega_0) + (1 + n_i)\delta(\omega - \omega_0)]. \tag{6}$$

It is interesting to note that $G^{-+}(\omega) \neq 0$ ($G^{+-}(\omega) \neq 0$) when $\omega < E_{FL}(\omega > E_{FR})$ at $T = 0$, while $\Sigma^{-+}(\omega) \neq 0$ ($\Sigma^{+-}(\omega) \neq 0$) when $\omega < E_{FL} - \hbar\omega_0(\omega > E_{FR} + \hbar\omega_0)$. This implies using the relation

$$2\,\mathrm{Im}[\Sigma_i^{R}(\omega)] = \Sigma_i^{-+}(\omega) - \Sigma_i^{+-}(\omega) \tag{7}$$

that, in the interval $E_{FR} < \omega < E_{FL}$, $\mathrm{Im}[\Sigma_i^{R}(\omega)] \neq 0$ when $E_{FL} - E_{FR} > \hbar\omega_0$, which establishes the condition for a real inelastic optical phonon process to occur. For an applied bias less than this limit, inelastic scattering is controlled by acoustic phonons which in general interacts more weakly with the electronic degrees of freedom. As a

consequence it is possible to say that the applied bias together with the temperature are the relevant variables to regulate the electron–phonon effect on transport.

The self-energy $\Sigma_i^R(\omega)$ can be obtained using equations (5) and (7). It yields

$$\mathrm{Im}[\Sigma_i^R(\omega)] = -(V_i^2/8\pi)\{[G_{ii}^{+-}(\omega-\omega_0) - G_{ii}^{-+}(\omega+\omega_0)]/2 + 2n_i\,\mathrm{Im}[G_{ii}^R(\omega-\omega_0) + G_{ii}^R(\omega+\omega_0)]\} \tag{8a}$$

and Hilbert transforming this equation gives

$$\mathrm{Re}[\Sigma_i^R(\omega)] = -\frac{V_i^2}{8\pi}\left(\omega_0\int_{-\infty}^{\infty}\frac{G_{ii}^{+}(E)\,\mathrm{d}E}{(E-\omega)^2-\omega_0^2} - (1+n_i)\,\mathrm{Re}[G_{ii}^R(\omega-\omega_0)] + n_i\,\mathrm{Re}[G_{ii}^R(\omega+\omega_0)]\right) \tag{8b}$$

where we have used the relation

$$2\,\mathrm{Im}[G_{ii}^R(\omega)] = G_{ii}^{-+}(\omega) - G_{ii}^{+-}(\omega). \tag{9}$$

Knowledge of the self-energies permits one to obtain the Green functions of the system and all its physical properties that we are interested in.

4. The electrical current density

In figure 1 we have represented the two heterostructures that we have studied. The total current density crossing the sample is obtained as the thermodynamical non-equilibrium mean value of the current density operator. This mean value can be obtained by calculating the probability that an electron hops from site i to site $i+1$, minus the probability of the reverse process. As there are no sources or sinks of electrons in the system, the result is independent of the particular choice of site i. For the Keldysh formalism this is true if the perturbation expansion from the state for which the system is partitioned is done to all orders of perturbation theory. As the choice is a matter of convenience, it will be made at the contact between the left lead and the heterostructure, involving the sites 1 and 2 shown in figure 1. The mean value of the current density is then given by

$$J = (\mathrm{i}e/\hbar)t_{12}(\langle c_{1\sigma}^{+}c_{2\sigma}\rangle - \langle c_{2\sigma}^{+}c_{1\sigma}\rangle) \tag{10}$$

where sites 1 and 2 are linked by the one-particle hopping t_{12}.

In order to calculate the non-equilibrium mean values appearing in equation (10) we apply the formalism presented in the last section. After some algebra, using equations (3) and (10) the total current density can be obtained as the sum of two contributions:

$$J_{\mathrm{el}} = \frac{et_{12}^2t_{N-1;N}^2}{2\pi\hbar}\int g_{11}^{-+}(\omega)g_{NN}^{+-}(\omega)|G_{N-1;2}^R(\omega)|^2\,\mathrm{d}\omega \tag{11a}$$

$$J_{\mathrm{inel}} = \frac{\mathrm{i}et_{12}^2t_{N-1;N}^2}{4\pi^2\hbar}\sum_j V_j^2\int |G_{2j}^R(\omega)|^2\,|G_{N-1;j}^R(\omega')|^2 g_{11}^{-+}(\omega) \times g_{NN}^{-+}(\omega')D_j^{+-}(\omega-\omega')\,\mathrm{d}\omega\,\mathrm{d}\omega' \tag{11b}$$

$$J_T = J_{\mathrm{el}} + J_{\mathrm{inel}} \tag{11c}$$

where N is the number of layers which compose the sample. As is evident from equation (3*d*) for the undressed Green functions $g_{ij}^{-+}(\omega)$ and $g_{ij}^{+-}(\omega)$, integration of equation (10) is restricted to the interval $E_{FL} - E_{FR}$ which guarantees that the current density is zero when there is no external applied bias. J_{el} describes processes in which the electron participating in the conduction excites a virtual phonon without changing its total energy. The inelastic contribution given by equation (11*b*) refers to a situation in which a real phonon is emitted or absorbed and an electron tunnelling through the structure loses or increases its energy. The convolution between the electron and phonon propagators in equation (11*b*), indicates this situation. For the case of an optical phonon, using equation (5), equation (10*b*) can be rewritten as

$$J_{inel} = \frac{et_{12}^2 t_{N-1,N}^2}{2\pi\hbar} \sum_j V_j^2 \{ |G_{2j}^R(\omega)|^2 g_{11}^{-+}(\omega)[(1+n_j)|\,|G_{N-1,j}^R(\omega-\omega_0)|^2 + n_j\,|G_{N-1,j}^R(\omega+\omega_0)|^2\, g_{NN}^{+-}(\omega+\omega_0)]\,d\omega. \quad (12)$$

When the system is at $T = 0$, so that $n_j = 0$, equation (11) gives a contribution if $E_{FR} + \hbar\omega_0 < E_{FL}$, indicating that for an inelastic process to take place the scattered electron needs an empty state to go to.

The total current density given by equation (3*c*) has been calculated at the edge of the heterostructure between the sites 1 and 2 in figure 1. Its value, as already mentioned, is site independent. The elastic and inelastic current densities are, however, site dependent in the region where the electron–phonon interaction operates, while they are site independent outside it. Note that, in order to calculate the effect that the inelastic processes have on the total current density, the elastic and inelastic contributions have to be calculated outside the heterostructure, in the region where the carriers (electrons or holes) have already passed through the sample.

5. Transport in a double-barrier heterostructure

Since the dominant electron–phonon interaction in polar semiconductors involves longitudinal optical phonons, we neglect the effect of acoustic phonons in the study of the tunnelling properties of the structure. Certainly for $E_{FL} - E_{FR} > \hbar\omega_0$ this is completely justified. The electron–phonon interaction is supposed to be active in the well region. As is well known, double-barrier heterostructures possess slab phonons: bulk-like-confined and interface phonon modes (Ridley, 1989; Jain and Das Sarma, 1989). Since the electronic wavefunction is small and the phonon is exponentially localized at the interface, the electron–interface phonon interaction is weak and can be neglected. As far as bulk-like phonons are concerned, the main effect originating from confinement is to introduce selection rules imposed by symmetry which leads to a reduction in the effective electron–phonon interaction. This effect can be incorporated in our model by simply renormalizing the strength of the interaction.

As the first example, we study a symmetric 1D heterostructure. Not only has the analysis of 1D systems academic interest. Recently (Ridley 1989), peaks observed in the resonant tunnelling of GaAs($Al_xGa_{1-x}As$/GaAs heterostructures have been attributed to confinement in a perpendicular direction to the current density, which corresponds for each peak to a quasi-one-dimensional system. Typical values of the electron–optical phonon interaction strength are $0.1 < g < 0.5$ where g is defined by $g = (V_i/\hbar\omega_0)^2$.

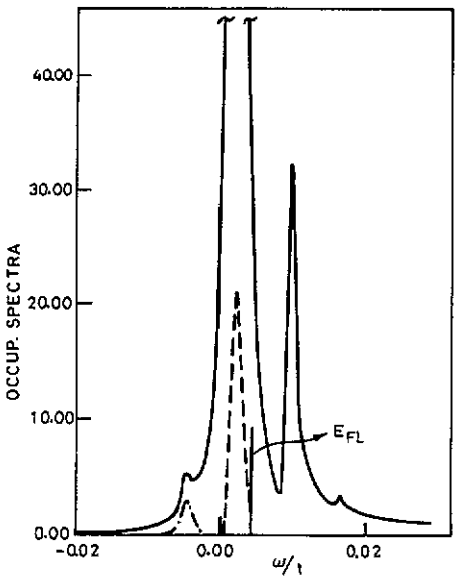

Figure 2. Local density of states (———) at the middle of the well discussed in the text for $T = 0$, $E_{FL} = 20$ meV and $\Delta V = 300$ meV. – – –, occupation spectra.

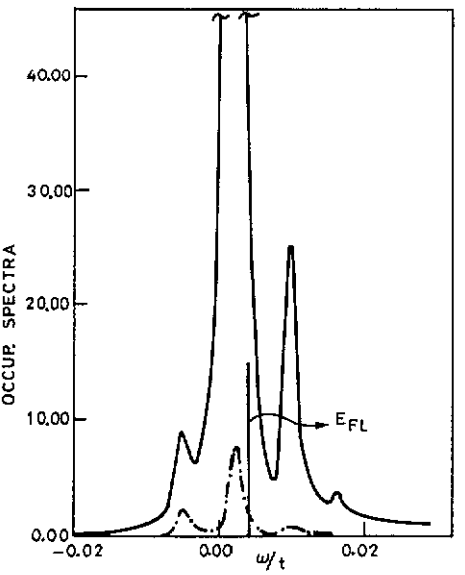

Figure 3. As figure 2 for $T = 300$ K.

The heterostructure is assumed to be constituted of barriers of nine atoms and a well of ten atoms with barrier heights between 40 and 400 meV, which in fact correspond to structures of $GaAs/Al_xGa_{1-x}As/GaAs$ with different values of x. The effective mass m^* which determines the value of $t = 5.2$ eV is taken to be $m^* = 0.067$ and the optical phonon frequency $\hbar\omega_0 = 36$ meV. The Fermi energies are obtained for two different situations: $E_{FL} = 20$ meV and 70 meV and $E_{FR} = E_{FL} - \Delta V$, where ΔV is the external applied bias.

In figure 2 we show the local density of states and the occupation spectra at $T = 0$ at the middle of the well for $g = 0.5$, $E_{FL} = 20$ meV and an applied bias $\Delta V = 300$ meV, which corresponds to the value for which the system is at resonance.

The appearance of two polaron peaks to the right and one to the left of the main peak is clear. These quasi-particle excitations correspond to the dressed electron and hole densities of the main peak due to the cloud of emitted phonons, since at zero temperature the carriers can only emit phonons. The electron-like peak (the one on the left) is much smaller than the first on the right because the occupation electron density of the main peak is small compared with the occupation hole density. This is seen in the occupation spectra presented in the same figure 2. According to equations (3*a*) and (3*b*), this occupation spectra can be split into elastic and inelastic contributions. The elastic contribution extends from 0 to E_{FL}, while the inelastic contribution appears below $E = 0$; this case corresponds to the electrons that have relaxed their energy by the emission of a phonon, so that they are filling the electron-like peak which appears below the main peak. The n-phonon processes for $n > 1$ are almost negligible for the electron–phonon interaction strength used to calculate figure 2.

In figure 3 we show the same case as in figure 2 but for $T = 300$ K. Two thermal effects are worthwhile mentioning. The two polaron peaks around the main peak are

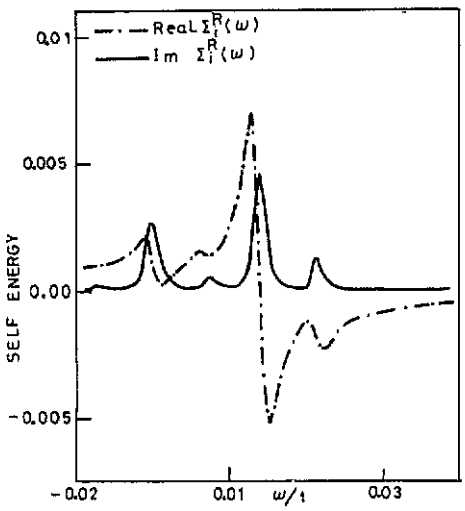

Figure 4. Self-energy as a function of ω for the case of figure 2. $-\cdot-$, $\mathrm{Re}[\Sigma_i^R(\omega)]$; ———, $\mathrm{Im}[\Sigma_i^R(\omega)]$.

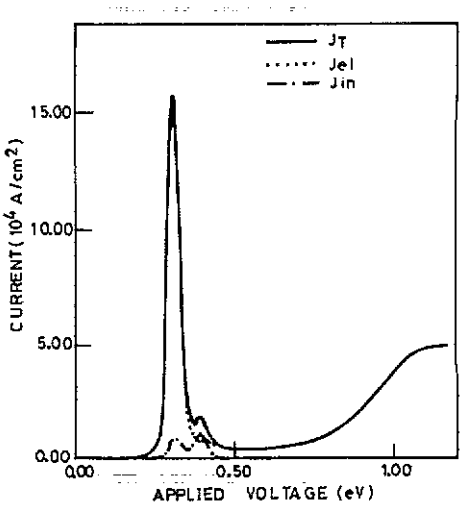

Figure 5. J–V characteristics for the case of figure 2. The total current density J_T (———) is split into its elastic part J_{el} (. . . .) and inelastic part, J_{inel} (– · –)

now more similar to each other because of the existence of thermal excited phonons in the sample; the temperature increase makes the spectra more symmetric around the main peak since the emission and absorption parts are proportional to $1 + n_i$ and n_i, respectively (n_i being the number of phonons in the i site). On the other hand, owing to thermal excitations both the elastic and the inelastic occupation spectra have contributions above E_{FL}. Now, in the case $T \neq 0$ we find that inelastic contributions associated with electrons have increased their energy by the absorption of a phonon, so that they are partially filling the peak appearing $\hbar\omega_0$ above the main peak.

It is worth mentioning at this point that similar polaron peaks due to optical phonons have been found recently by Cai *et al* (1989) who have calculated the transmission coefficient of an electron through a double barrier in the presence of electron–optical phonon scattering. The Keldysh method allows us to calculate the total current density, the occupied electron density of states and also other related properties discussed below.

The peaks in the density of states represent excited polaron states of the system with a lifetime given by $\mathrm{Im}[\Sigma_i^R(\omega)]$. The self-energy as a function of ω is given in figure 4 for the same sample described before. From the figure we obtain that the lifetime of the polaron at resonance is of the order of 10^{-13} s, while the electronic tunnelling times that can be obtained from figure 2 are of the order of 2×10^{-14} s. This is the reason why only a small fraction of the electronic occupation spectra appears below the incident energy. The electrons go through the well too rapidly for it to be possible for them to relax through the emission of an optical phonon. This situation is clearly seen in figure 5 where we show the J–V characteristics at $T = 0$. The elastic and inelastic contributions to the total current density are shown explicitly. The tunnelling is essentially an elastic phenomenon in this case. However, this depends upon the applied voltage and in particular, for an applied voltage corresponding to the emission of a phonon, inelastic processes are more important than elastic processes. Tunnelling is here partially elastic and partially sequential. The electron enters into the well elastically, it reduces its

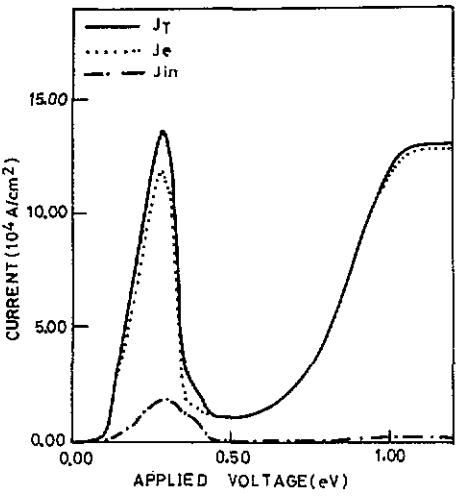

Figure 6. *J–V* characteristics for the case of figure 3. The total current density, J_T (———) is split into its elastic part J_{el} (. . . .) and inelastic part J_{inel} (– · –).

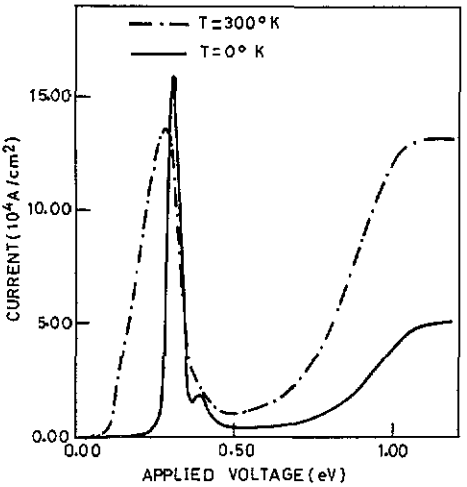

Figure 7. Total current density as a function of the applied voltage for the cases in figure 2 ($T = 0$) (———) and figure 3 ($T = 300$ K) (– · –).

energy by the emission of a phonon and then it continues its trajectory outside the heterostructure. This aspect of the problem will be discussed in more detail below. The phonon-side band peak of the elastic current density coming from polaronic excitations is very small. The phonon absorption peak is non-existent because at $T = 0$ there are no phonons in the system. The phonon-emission-assisted tunnelling represented by the inelastic contribution to the current density has an applied bias threshold of $E_{FL} - E_{FR} > \hbar\omega_0$ as is apparent in figure 5.

In figure 6 we present the *J–V* characteristics of the same system for $T = 300$ K. The main difference from the results already analysed is the large broadening of the resonant peak. The reasons for this behaviour are essentially two: the first is the promotion of electrons to higher energies as they absorb phonons in the thermal bath, and the second is the existence of available thermally excited electrons which energetically match the resonance condition for a much lower applied voltage. The disappearance of the resonant peak is produced by an applied voltage such that the energy level of the localized state at the well goes beyond the bottom of the conduction band of the emitter. This condition is independent of temperature as can be observed by comparing figures 5 and 6. Inelastic processes are favoured owing to the increase in the phonon population with increasing temperature. The inelastic contribution to the current density rises in comparison with the $T = 0$ case. The side-band peak loses definition and the current density increases rapidly with increasing applied voltage in the out-of-resonance region owing to the presence of more energetic electrons which are capable of participating in the transport process.

Direct comparison of the total current density as a function of applied voltage for the cases $T = 0$ and $T = 300$ K can be seen in figure 7.

In order to study the effect that the tunnelling well time has on the non-equilibrium electronic population we have compared in figure 8 the occupation spectra at the middle of the well for various heterostructures which differ only in the barrier height (the barrier

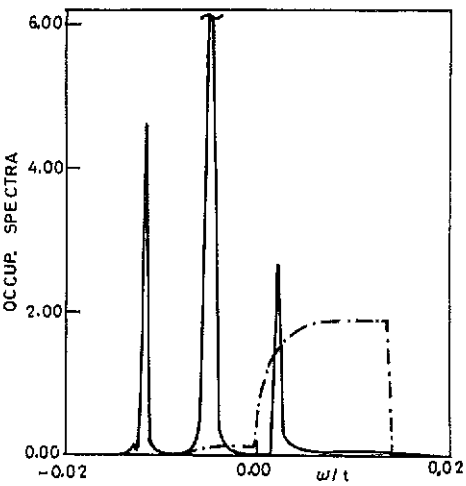

Figure 8. Occupation spectra at the middle of the well discussed in the text for two heterostructures having different barrier heights: ———, the barrier height is 600 meV; – · –, the barrier height is 100 meV.

height controls the time that the electron spends in the well before escaping). The applied bias is such as to have the first polaron side-band peak in resonance for $E_{FL} = 70$ meV. It is clear from the figure that, for the case of a barrier height $E_1 = 100$ meV, the electrons go through the heterostructure essentially without suffering an inelastic collision. The electronic population at the centre of the well is almost contained between the bottom of the conduction band and the Fermi energy E_{FL} of the emitter. On the contrary for the sample with $E_1 = 600$ meV, as the electrons are reflected many times back and forth in the barrier, the real path is in this case longer than the mean free path for inelastic collisions and, as a consequence, almost all electrons have released their energy through one or two scattering phonon processes to the region below the bottom of the conduction band of the emitter.

For the sake of completeness we have calculated the J_T–V characteristics for a 3D sample. The problem can be mapped onto a 1D situation by simply Fourier transforming along the direction perpendicular to the current; thus, we recover a 1D Hamiltonian with parameters depending upon $k_\parallel$. We suppose, as already mentioned, that the dispersion relation for the optical phonon is completely flat and that the electron–phonon interaction is independent of $k_\parallel$. For small values of $E_{FL} = 20$ meV the shape of the J_T–V curve is almost the same as in the 1D case; for greater values of E_{FL} the curve broadens and adopts the well known triangular shape, and the satellite peak is less distinguishable.

We have calculated the influence of including the electron–phonon coupling along the barriers. For the case of AlGaAs there are two optical phonons involved in the problem at 35 meV and 47 meV. The J_T–V characteristic suffers only very small effects and there is no evidence of a peak located at 47 meV although we have adopted the same value for $g = 0.5$ as in the well region. This result is a consequence of the fact that the density of states at the barriers is much less than at the well and there are not enough electrons to induce the emission of a phonon. It is likely that the assignment of the satellite peak, detected experimentally (Goldman *et al* 1987a, b) for GaAs/AlGaAs/GaAs, to emitted phonons at the barriers, is not appropriate.

6. Multiphonon process in semiconductor microchannels

The C–V characteristics of metal–semiconductor contacts and capacitors of GaAs/$Al_xGa_{1-x}As$ show periodic structures (Hickmott *et al* 1984, Lu *et al* 1985). This behaviour

has been explained by multiphonon processes that take place when carriers under the effect of an applied bias move along the channel. Kulik and Shekhter (1983) have treated the problem of a narrow semiconductor channel of width d theoretically, where d is much smaller than the channel length L and λ_a, the mean free path due to acoustic phonons. The theory is based on Boltzmann equation formalism and predicts a C–V curve that has singularities when the applied voltage: $\Delta V = \hbar\omega_0$. These singularities result from an n-phonon emission event. Although the experimental behaviour is not singular, this theory provides a qualitative description of the multiphonon processes.

In order to show the applicability of the microscopic theory developed here to describe this type of phenomena, we have studied the electrical current of a linear chain in contact with two reservoirs of electrons having Fermi levels E_{FL} and E_{FR} represented by two Bethe lattices of coordination 3. This idealized model approximately describes the situation of the system in which we are interested, as is schematically shown in figure 1(b). Although we have taken a very simple model, the inclusion of more sophisticated and realistic conditions does not generate serious difficulties in the calculation.

In order to have multi-optical-phonon processes, the condition $L \gg \lambda_0$ has to be satisfied, where λ_0 is the mean free path due to optical phonons. In this case, electrons can suffer an n-phonon process as they go along the sample, with the maximum value of n such that $n \simeq \Delta V/\hbar\omega_0$, ΔV being the potential drop in the chain.

For $L \gg \lambda_0$ the linear chain has an ohmic resistance; for an applied voltage, it is appropriate to assume that the potential profile has a linear site dependence within the chain. For simplicity we assume that the contact resistance is zero, although this is not necessarily the case. The only significant effect of the contact resistance is that the oscillations seen in the conductance have a period longer than ω_0 (this in fact corresponds to the experimental result) owing to the potential drop at the contacts. However, the contacts have a more significant effect, related to the quantum oscillations of the conductance as a function of the applied voltage because of the existence of standing waves produced by reflections at the contacts. These oscillations might mask the relatively smaller oscillations due to multi-phonon processes. Fortunately in real systems this behaviour is not detected because the microchannels are not well defined and the potential profile is smooth at the edges. This situation can be simulated for the simple model that we are considering by supposing that the coordination number of the Bethe lattice reservoirs varies smoothly along several atoms from the chain value $Z = 2$ up to $Z = 4$. Twenty atoms are sufficient to eliminate the quantum interference oscillation of a linear chain constituted by 200 atoms in a situation in which the system is free of electron–phonon interactions. This guarantees that all possible oscillation effects are due to electron–phonon interaction.

In our calculation, we take $E_{FL} = 0.01t$, $E_{FR} = E_{FL} - \Delta V$ and $\hbar\omega_0 = 0.007t$ which corresponds to the phonon energy for GaAs ($t = 5.27$ eV). We also take the electron–phonon strength $g = 4$, which has been chosen such that $L \gg \lambda_0$, where

$$\lambda_0 = \frac{\hbar k_F}{m^* \operatorname{Im} \langle \Sigma^R(\omega) \rangle}$$

($\langle \Sigma^R(\omega) \rangle$ being the mean value of $\Sigma^R(\omega)$ in the interval (E_{FL}, E_{FR})); k_F is the Fermi momentum, and $\hbar k_F = (0.02tm^*)^{1/2}$ and $m^* = 0.067$ for GaAs.

In figure 9 we show the J_T–V and dJ_T/dV–V curves. Although the current density oscillations are small, its derivative shows clear oscillations. When the applied voltage increases so as to allow for a subsequent phonon process, the self-energy of equation (4)

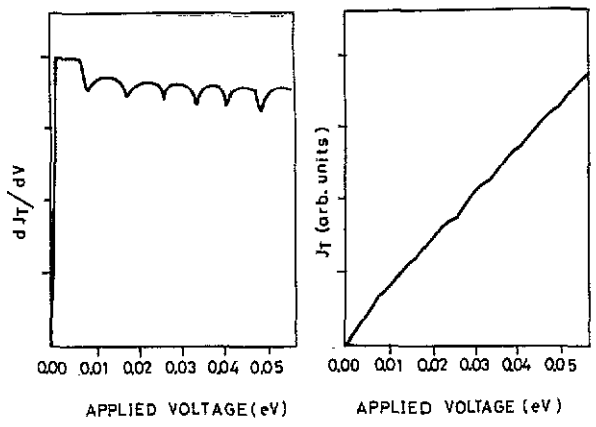

Figure 9. J_T and dJ_T/dV–V curves for the microstructure discussed in the text.

has an extra renormalization (this occurs because the propagator in equation (4) is a completely dressed self-consistent object). This is reflected in a small oscillation in the conductivity due to the appearance of an extra channel for the electrons through the emission of a new phonon. Although it is not possible to make a direct comparison with the experiments, the theoretical results obtained here are similar, and the general shape of the curves equivalent, to the experimental measurements obtained for microchannels of $In_xGa_{1-x}As$ (Lu *et al* 1985).

7. *Summary and conclusions*

We have addressed the effect that electron–phonon inelastic scattering has on the properties of mesoscopic semiconducting structures. We have used a Green function formalism based on the Keldysh diagrammatic expansion. This formalism has shown to be particularly suitable for analysing a situation where the many-body system is under the effect of a large applied voltage and as a consequence very far from equilibrium.

In the last few years, a very elegant transport theory has been developed which considers the sample to be connected to inelastic scatterers which randomize the phase of the electronic wavefunction (Büttiker 1986). Although this phenomenological theory has contributed to clarification of many aspects of the inelastic scattering, we think that there is still a lack of a microscopic theory capable of describing in detail the different kinds of inelastic event that an electron suffers under the effect of an external bias. This requires use of a many-body theory to study the current as well as other non-equilibrium properties of the system, i.e. the occupation spectrum which it is essential to know if we were interested, for instance, in the optical properties of the system. This paper is an effort in this direction. We have studied the effects of the electron–phonon interaction, in particular for the case of a double-barrier heterostructure and a mesoscopic constriction. Although we have adopted simple models, we have obtained results which compare well with the experimental measurements. Full quantitative agreement of the theory with the experiments (current intensity, peak-to-valley ratio, etc) would require a more realistic microscopical model including, within the context of a self-consistent Hartree–Fock approximation for the electron–electron interaction, the potential profile as a function of position. It is well known that the interesting bistable behaviour (Goldman *et al* 1987a, b) observed in double-barrier structures is due to a charge-generated potential

which being non-linear gives rise to more than one solution for the J_T–V characteristics. We have assumed for the systems analysed here that the potential profile is linear as a function of position along the current direction. Although this is perfectly justified for the linear microchannel, in the double-barrier case, as the system is heterogeneous and the charge is unequally distributed, this assumption is not always realistic.

The self-consistent treatment of the electron–electron interaction in order to study the effect of a non-linear potential profile and the metal–insulator transition due to electronic correlation will be the subject of a future publication.

Acknowledgments

Financial support by the Spanish CAICYT and the Ministerio de Educación y Ciencia is gratefully acknowledged. This work was partially supported by the Universidad Federal Fluminense and the Brazilian CNP.

References

Büttiker M 1986 *Phys. Rev.* B **33** 3020
—— 1988 *IBM J. Res. Dev.* **32** 317
Cai W, Zheng T F, Hu P, Yudanin B and Lax M 1989 *Phys. Rev. Lett.* **63** 418
Caroli C, Combescot R, Nozieres P and Saint-James D 1971 *J. Phys. C: Solid State Phys.* **4** 916
—— 1972 *J. Phys. C: Solid State Phys.* **5** 21
Chen L Y and Ting C S 1990 *Phys. Rev.* B **41** 8533
D'Amato J L and Pastawski H M 1990 *Phys. Rev.* B **41** 7411
Datta S 1990 *J. Phys.: Condens. Matter* **2** 8023
Goldman V J, Tsui D C and Cunningham J E 1987a *Phys. Rev.* B **36** 7635
—— 1987b *Phys. Rev. Lett.* **58** 1256
Hickmott T W, Salomon P M, Fang F F, Stern Frank, Fischer R and Morkoc H 1984 *Phys. Rev. Lett.* **52** 23
Jain J K and Das Sarma S 1989 *Phys. Rev. Lett.* **62** 2305
Jonson M 1989 *Phys. Rev.* B **39** 5924
Keldysh L V 1965 *Sov. Phys.–JETP* **20** 1018
Kulik I O and Shekhter R J 1983 *Phys. Rev. Lett.* A **98** 132
Landauer R 1989 *J. Phys. C: Solid State Phys.* **1** 8099
Lu P F, Tsui D C and Cox H M 1985 *Phys. Rev. Lett.* **54** 1563
Migdal A B 1958 *Sov. Phys.–JETP* 7 996
Pernas P L, Martín-Rodero A and Flores F 1990 *Phys. Rev.* B **41** 11
Ridley B R 1989 *Phys. Rev.* B **39** 5282
Shah J 1986 *Quantum Electron.* **22** 1728
Wingreen N, Jacobsen K W and Wilkins J W 1989 *Phys. Rev.* **40** 11834
Yuming H 1988 *J. Phys. C: Solid State Phys.* **21** L23